33rd Annual International Conference of the IEEE EMBS
Boston, Massachusetts USA, August 30 - September 3, 2011

A Critical Review of the Effects of De-noising Algorithms on MRI Brain Tumor Segmentation

Idanis Diaz, Pierre Boulanger, Russell Greiner, and Albert Murtha

Abstract— **One can find in the literature numerous techniques to reduce noise in Magnetic Resonance Images (MRI). This paper critically reviews modern de-noising algorithms (Gaussian filter, anisotropic diffusion, wavelet, and non-local mean) in terms of their efficiency, statistical assumptions, and their ability to improve brain tumor segmentation results. We will show that although different techniques do reduce the noise, many generate artifacts that are incompatible with precise brain tumor segmentation. We also show that the non-local means algorithm is the best de-noising technique for brain tumor segmentation.**

I. Introduction

Magnetic Resonance Images (MRI) are widely used for diagnosis and the treatment of brain tumors. MRI provide invaluable information about localization, shape, and size of tumors without exposing the patient to a high ionization radiation as with other modalitie like: CT, PET, or SPEC. However, during the MRI acquisition process there are trade-offs between resolution, acquisition speed, and signal-to-noise ratio (SNR) that affect image quality and its subsequent analysis. One way to improve the SNR in MRI is to increase the acquisition time. Although such an option is not always practical due to technical limitations and patient comfort. In general, when the acquisition time is reduced and the temporal resolution is increased, both the SNR and the contrast are degraded. Noise and low-contrast in MRI data make it difficult to precisely delineate regions of interest between tumor and normal brain tissues. Most segmentation algorithms found in the literature [1] tend to be very sensitive to noise, intensity inhomogeneities and low-contrast. For this reason, it is necessary to pre-process MRI data to reduce noise and to enhance contrast between regions. There are several algorithms proposed for de-noising MRI data, some adapted from general image processing methods while others developed specifically to deal with the noise in MRI. Some authors [2], [3], [4], argue that MRI should be treated differently because the noise does not follow the standard Gaussian assumption, but a more complex Rician distribution [5]. It is well known that almost all image processing filters are based on the Gaussian assumption and do blur discontinuities between regions hence, reducing contrast. This is the main challenge in de-noising MRI data for a segmentation application, i.e. to preserve the edges and details but at the same time to reduce noise in uniform regions. There are many algorithms described in the literature capable of reducing MRI noise and hence improving the SNR. On the other hand there is no comprehensive review comparing their abilities at improving the quality of the data such as high spatial resolution and good contrast, and also improving segmentation and visualization. One can divide the MRI de-noising algorithms into four major categories: Finite Impulse Filters (FIR), Anisotropic Diffusion, Wavelet, and Non-Local Means (NLM) algorithms.

This paper is organized as follows, Section II briefly explains the basic principles of each category. Section III, describes the experiments carried out to compare the different algorithms at de-noising MRI data and improving image quality for brain tumor segmentation. Section III discusses the results, and finally, Section IV concludes and presents future research directions.

II. De-noising Algorithms

In this section, we explain the basic principles for three main algorithms, Anisotropic Diffusion, Wavelets, and Non-Local Means. In this section we will omit Gaussian filter as it is trivial.

A. Algorithm Based on Anisotropic Diffusion

Anisotropic diffusion was first introduced by Perona and Malik [6] as a multi-scale technique to detect edges. The algorithm is based on an anisotropic diffusion process that favors smoothing within continuous regions while it avoids smoothing across boundaries between regions. The filter is based on a constrained differential diffusion equation where pre-computed edges are viewed as locations with low diffusion coefficients. The diffusion equation is:

$$I_t = \mathrm{div}(c(x,y,t)\nabla I) = c(x,y,t)\triangle I + \nabla c \cdot \nabla I \qquad (1)$$

The operators div, ∇ and $\triangle$ are the divergence, the gradient and the Laplacian operators respectively. I represents an intensity image while t is the process ordering parameter or diffusion time. The term $c(x,y,t)$ is a scalar field controlling the diffusion strength. It has a monotonically decreasing function that is directly proportional to the initial magnitude of the gradient $\triangle I$. At locations with large gradients, where boundaries are assumed to happen, the initial value of $c(x,y,0)$ is close to zero while it is a maximum at locations with small gradients.

I. Diaz is at Dept. of Comput. Science, U. of Alberta, Canada and *U. del Magdalena*, Colombia, idanis@ualberta.ca

P. Boulanger and R. Greiner are at Dept. of Comput. Science, U. of Alberta, Canada, pboulanger, rgreiner@ualberta.ca

A. Murtha is at The Cross Cancer Inst., U. of Alberta, Canada, albert.murtha@albertahealthservices.ca

Perona and Malik propose the following equations to estimate the values of $c(x, y, t)$:

$$g(\nabla I) = \exp\left(-\left(\|\nabla I\|/K\right)^2\right) \quad (2)$$

or

$$g(\nabla I) = \left(1 + \left(\|\nabla I\|/K\right)^2\right)^{-1} \quad (3)$$

where K is a scalar parameter controlling the edge enhancement threshold.

B. Algorithm Based on Wavelet Analysis

Wavelets and multi-resolution analysis are intrinsically connected. Multi-resolution analysis with wavelets is based on two operations: dyadic dilations and integer translation [7]. The Wavelet transform has the advantage of being adaptable in both time and frequency to discontinuities in the signal. In the wavelet framework, a signal $f(x)$ is represented as infinite combinations of a discrete wavelet at different scales and translations as defined by:

$$f(x) = \sum_{j=-\infty}^{\infty} \sum_{k=-\infty}^{\infty} d_{j,k} \Psi_{j,k}(x). \quad (4)$$

In Equation (4), j and k are the scale and translation parameters respectively. The function $\Psi_{j,k}(x)$ is called a *mother wavelet* or basis function at scale j with a distinct translation k. The coefficients $d_{j,k}$ $\{j, k \in \mathbb{Z}\}$ called the wavelet or mixing coefficients of $\Psi_{j,k}(x)$ are used to reconstruct $f(x)$. Each coefficient $d_{j,k}$ is estimated by convolving the signal $f(x)$ with the *mother wavelet* function $\Psi_{j,k}(x)$:

$$d_{j,k} = \int_{-\infty}^{+\infty} f(x) \Psi_{j,k}(x) dx = \langle f, \Psi_{j,k}(x) \rangle. \quad (5)$$

With wavelet analysis, the signal's energy is distributed through out the scale-space. De-noising in the wavelet-scale domain involves thresholding the coefficients $d_{j,k}$ at different scales and discarding those with non-significant energy that do not change the signal's morphology.

C. Algorithm Based on Non-Local Means

The de-noising methods in this category were first introduced by Buades, Coll, and Morel [8]. In principle, these algorithms estimate the true value at pixel i from the mean of all the values from non-local pixels or voxels whose neighborhoods are similar to the neighborhood of i. Given a discrete image $\upsilon = \{\upsilon(i) \,|\, i \in I\}$, the estimated value $\mathrm{NL}[\upsilon](i)$ is computed as a weighted average of all the pixels j in the image:

$$\mathrm{NL}[\upsilon](i) = \sum_{j \in I} w(i, j) \upsilon(j) \quad (6)$$

In Equation (6), each $w(i, j)$ is a weight that depends on the similitude metric between grey levels of the neighborhoods around pixels i and j. The similitude between two neighborhoods is estimated using a Gaussian weighted Euclidian distance.

III. Experiments and Results

The comparison among methods presented in this section was performed on twenty simulated T1-MRIs. This set of images were generated using the brain MRI simulator, BrainWeb [9]. We also used ten real MRIs containing brain tumors to see the effect of the filters on tumor segmentation. These MR images were provided by the Brain Tumor Analysis Project [10], a joint project between the Cross Cancer Institute and the Computing Science Department at University of Alberta, Canada. We compared six algorithms from the four categories: Gradient anisotropic diffusion algorithm implemented by Gerig et al. [11], curvature anisotropic diffusion implemented in the ITK library, an open-source, cross-platform image processing library that provides software developers tools for image processing [12], Nowak's method based on wavelet [2], the original non-local means algorithm proposed by Buades et al. [8], the unbiased non-local means algorithm proposed by Manjón et al. [3], and finally, a simple Gaussian filter as a reference.

A. Evaluation for Synthetic MRIs

The brain MRI simulator in [9] allows the user to generate synthetic MR brain images with different modalities, levels of noise, slice thickness, and non-uniformity contents. We first generated a complete volume without noise as our reference. This reference volume contains 20 slices of 5 mm. thick and it is generated with "Inversion Recovery" (IR) scan technique to generate slices similar to the real MRIs data that we also used in our evaluation. Each 2-D image is corrupted with Rician-noise for ten different values of variance σ_i in the range between $[2, 20]$. We compared the performance of the different algorithms in the least-square sense using the Root-Mean-Square Error (RMSE), Equation (7):

$$\mathrm{RMSE} = \sqrt{(\upsilon_o - \upsilon_f)^2} \quad (7)$$

where υ_o is the noise-free image and υ_f is the smoothed image. Figure (1a) and Figure (1b) illustrate the performances of each algorithm. The horizontal axis in each figure represents the noise variance σ while the vertical axis is the logarithm of average RMSE values obtained for each method over the set of twenty MR images. Figure (1a) shows that Nowak's method had the worst performance of all methods tested. The two anisotropic diffusion algorithms and the Gaussian filter showed similar performance at different noise levels. Figure (1b) depicts the performance of the two non-local mean algorithms and the Gaussian filter. The classical non-local means version performance is similar to the Gaussian filter, while Manjón's variant outperformed both the classical non-local means and the Gaussian filter.

Figure (2) shows de-noised slices. Figure (2a) is a synthetic MRI slice without noise, Figure (2b) is the same slice with noise at level $\sigma = 16$ and the remaining subfigures are the results obtained after applying each of the de-noising algorithms.

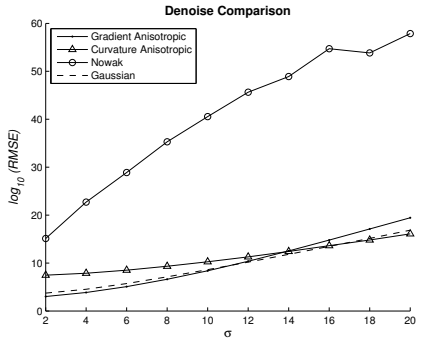

(a) Anisotropic algorithms vs. Nowak's algorithm vs. Gaussian filter

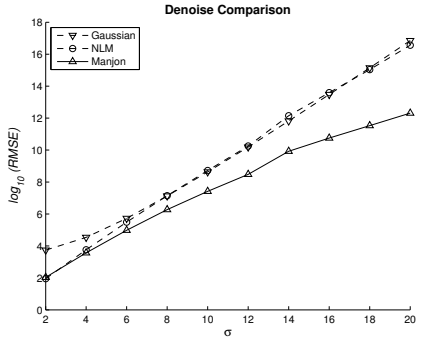

(b) Algorithms based on Non-local means vs. Gaussian Filter

Fig. 1: Performance comparisons at de-noising the synthetic images.

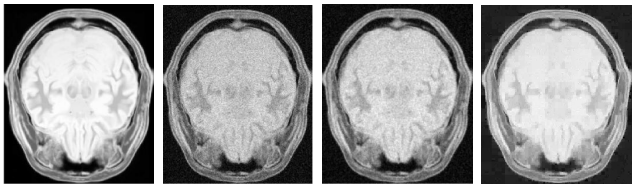

(a) Noise-free (b) Noise $\sigma = 16$ (c) Gaussian (d) Nowak

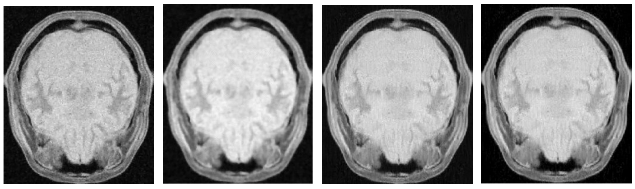

(e) Anisotropic (f) Curvature (g) NLM (h) Manjón

Fig. 2: Visual comparison for the various de-noising algorithms.

B. Evaluation for Real MRI Images

Next, we used Real MRI data to evaluate the algorithms performance for segmenting brain tumors. For this purpose, we used expert's manual tumor segmentation as references. The MRI segmentation was performed using the Confidence Connected Segmentation (CCS) algorithm in the ITK library [12]. First, we segmented the tumor on each unfiltered image in order to establish a performance baseline. We then performed the same segmentation after the image were processed by the six de-noising algorithms mentioned in Section III-A. The segmentation algorithm is tuned by the parameter f_{mult} that controls the inclusion of new pixels in the segmented area. Equation (8) shows the inclusion criterion:

$$\upsilon(X) \in [m - \sigma f_{\text{mult}}, m + \sigma f_{\text{mult}}] \tag{8}$$

where $\upsilon(X)$ is an image, X is the position of the neighboring pixel under consideration for inclusion in the current region, σ is the local neighborhood intensity values standard deviation. Equation (8) considers the standard deviation of a circular region around the mean of the current neighborhood. Neighboring pixels whose intensity values fall inside the range are accepted and are included to be part of the region. Then, both the mean and the standard deviation are updated after each iteration until no more pixels are available or the maximum number of iterations is reached [12]. The accuracy of each segmentation was evaluated using the Dice Similarity Coefficient (DSC), which measures the coincidence between two segmented regions [13]. Let two binary segmentations, $G(x, y)$ and $R(x, y)$ of an image υ, be the goal and resulting segmentations, the DSC is calculated as:

$$DSC(R, G) = \frac{2P\{(R(x, y) = 1) \bigcap (G(x, y) = 1)\}}{P(R(x, y) = 1) + P(G(x, y) = 1)} \tag{9}$$

where $R(x, y) = 1$ and $G(x, y) = 1$ represents the pixels inside of the target segmented areas in the two respective segmentations, in our case the target area is a tumor. The function P represents the segmentation probability.

We applied an ANOVA analysis within-subjects in order to determine if the segmentation results after de-noising are better than those without filtering. Our alternative hypothesis is that there is a difference between at least one of the segmentation results obtained after de-noising with one of the de-noising methods versus the results obtained without pre-processing. We considered two factors in the analysis: de-noising methods and the segmentation parameter f_{mult}. Ten real images were smoothed with the six de-noising algorithms. Afterwards, we applied the CCS segmentation algorithm with different values of $f_{\text{mult}} = 2.5, 2.65$ and 2.8 over the noisy and de-noised images. In total, we obtained 210 segmentations: 10 images $\times 7$ methods $\times 3$ values of f_{mult}.

The box-plot at Figure 3 summarizes the resulting means from the segmentation results for the different algorithms and the noisy image. We observe that the mean for Nowak's method is the least of the means from the de-noising methods, including the noisy version. When we include Nowak's method in the ANOVA analysis for the segmentation results, the alternative hypothesis was supported at 0.01 levels of significance with a $p_{0.01} = 0.0013$. However, when we exclude Nowak's method from the analysis, the alternative hypothesis is not longer supported with a $p_{0.01} = 0.9643$. Such results indicate that there are no differences in the segmentation results if we include a previous denoising step with the exception of Nowak's method.

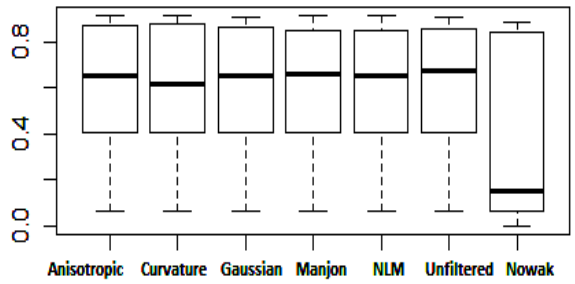

Fig. 3: Segmentation performance box-plot for each filtering method.

C. Discussion

Figures (1a) and (1b) show that Manjón's method, based on the non-local means algorithm and Rician noise distribution in MRIs, has the best performance. Other papers [3], [14] and [15], have also shown the superiority of non-local means over wavelet and anisotropic diffusion methods for de-noising MRI. Nowak's method had the worst performance at de-noising the set of synthetic images in Section III-A. However, the segmentation results obtained after de-noising with Nowak's showed a better contrast than the other methods. The main point of Nowak's work is to improve the contrast in the MRI. It seems that the contrast is improved at the expense of fidelity with the noise-free MRI. One reason for Nowak's low evaluation with the RMSE metric could be the effect of the Haar wavelet after the image reconstruction. When zooming on the results from Nowak's method one can see that the image is built with squared patches. Figure (1a) shows that the Gaussian performance closely follows the performance of both anisotropic algorithms.

Another isssue in MRI is that the edges between different tissues are not well defined since the contrast is low and contains no strong gradients between regions, thus the methods based on anisotropic diffusion do not have enough strength to stop at the boundaries of the regions and their results are similar to a Gaussian smoothing. These methods did not improve the quality of the MRI data for tumor segmentation. Our experiments show that although the methods did remove the noise from the MRIs, they do not improve the contrast and do not correct the inhomogeneities on the images enough to allow the region-growing based segmentation algorithms to stop when they should. Additionally, as Figure (2) shows, there are fine details and some edges lost in the de-noised images. Nowak's method improved the contrast of the images, however the segmentation has a hard time dealing with the small squared patches generated by the Haar wavelet on the image regions.

IV. Conclusion

The presence of noise and low-contrast in MRI make it difficult to perform visual inspections and computer-aided analysis of the images. In this work, we have evaluated the performance of the best algorithms proposed in the literature at de-noising MRI and at improving the quality of the data for brain tumor segmentation. We found that many of those algorithms do reduce noise without too much apparent artifacts, but our results show that they still blur the boundaries of the tissues, thus, the results of growing-region based segmentation algorithms are not improved after de-noising.

As future work, we will analyze if reducing noise on volumetric data, instead of slice-by-slice could improve the noise estimation and provide more information that allow us to reduce the noise and preserve the structure of the surfaces. Volumetric data provide redundant information for each voxel that can be used for a better discrimination of the noise. We will also study different methods to estimate the noise in the images.The blurring effect of the methods may be due to a poor estimation of the noise parameter on MRI.

References

[1] M. A. Balafar, S. Mashohor, A. R. Ramli, and M. I. Saripan, "Review of Brain MRI Image segmentation Methods," *Artif. Intell. Rev.*, vol. 33, no. 3, pp. 261–274, 2010.

[2] R. Nowak, "Wavelet-based Rician noise removal for magnetic resonance imaging," *IEEE Trans. Image Process.*, vol. 8, no. 10, pp. 1408–1419, October 1999.

[3] J. Manjón, J. Carbonell-Caballero, J. Lull, G. García-Martí, L. Martí-Bonmatí, and M. Robles, "MRI denoising using non-local means," *Med. Image Anal.*, vol. 12, pp. 514–523, February 2008.

[4] J. Sijbers, A. J. den Dekker, A. V. der Linden, M. Verhoye, and D. V. Dyck, "Adaptive anisotropic noise filtering for magnitude MR data," *Magn. Reson. Imaging*, vol. 17, no. 10, pp. 1533–1539, 1999.

[5] H. Gudbjartsson and S. Patz, "The Rician distribution of noisy MRI data," *Magnetic Resonance in Medicine*, vol. 34, no. 6, pp. 910–914, 1995.

[6] P. Perona and J. Malik, "Scale-space and edge detection using anisotropic diffusion," *IEEE Trans. Pattern Anal. Mach. Intell.*, vol. 12, no. 7, pp. 629–639, July 1990.

[7] R. T. Ogden, *Essential Wavelets for Statistical Applications and Data Analysis*. Boston: Birkhäuser, 1997.

[8] A. Buades, B. Coll, and J. Morel, "A non-local algorithm for image denoising," in *Proc. 2005 IEEE Conf. on Comp. Vis. and Patt. Recog. (CVPR'05)*, vol. 2, no. 11, 2005, pp. 60–65.

[9] McConnell Brain Imaging Centre of the Montreal Neurological Institute, "Brainweb: Simulated brain database," http://mouldy.bic.mni.mcgill.ca/brainweb/, 2006.

[10] R. Greiner, M. Brown, and A. Murtha, "Brain tumour analysis project," http://webdocs.cs.ualberta.ca/∼btap/, 2011.

[11] G. Gerig, O. Kubler, R. Kikinis, and F. Jolesz, "Nonlinear anisotropic filtering of MRI data," *IEEE Trans. Med. Imag.*, vol. 11, no. 2, pp. 221–232, June 1992.

[12] L. Ibañez, W. Schroeder, L.Ng, J. Cates, and the Insight Software Consortium, "The ITK software guide," November 2005.

[13] K. Zou, S. Warfield, A. Bharatha, C. Tempany, M. Kaus, S. Haker, W. Wells, F. Jolesz, and R. Kikinis, "Statistical validation of image segmentation quality based on a spatial overlap index," *Acad. Radiol.*, vol. 11, no. 2, pp. 178–189, 2004.

[14] Y. Gal, A. Mehnert, A. Bradley, K. McMahon, D. Kennedy, and S. Crozier, "Denoising of dynamic contrast-enhanced MR images using dynamic nonlocal means," *IEEE Trans. Med. Imag.*, vol. 29, no. 2, pp. 302–310, 2010.

[15] C. S. Anand and J. Sahambi, "Wavelet domain non-linear filtering for MRI denoising," *Magn. Reson. Imaging*, vol. 28, pp. 842–861, 2010.